

Articles

A New Double-Responsive Block Copolymer Synthesized via RAFT Polymerization: Poly(*N*-isopropylacrylamide)-*block*-poly(acrylic acid)

Christine M. Schilli,[†] Mingfu Zhang,[†] Ezio Rizzardo,[‡] San H. Thang,[‡] (Bill) Y. K. Chong,[‡] Katarina Edwards,[§] Göran Karlsson,[§] and Axel H. E. Müller*,[†]

Makromolekulare Chemie II, Universität Bayreuth, 95440 Bayreuth, Germany, CSIRO Molecular Science, Bag 10, Clayton South, Victoria 3169, Australia, and Department of Physical Chemistry, Uppsala University, Box 579, 75123 Uppsala, Sweden

Received December 4, 2003; Revised Manuscript Received July 23, 2004

ABSTRACT: Poly(*N*-isopropylacrylamide)-*block*-poly(acrylic acid), PNIPAAm-*b*-PAA, with low polydispersity was prepared by reversible addition–fragmentation chain transfer (RAFT) polymerization in methanol. The block copolymers respond to both temperature and pH stimuli. The behavior of the double-responsive block copolymers in solution was investigated by dynamic light scattering, temperature-sweep NMR, cryogenic transmission electron microscopy, and IR spectroscopy. The block copolymers form micelles in aqueous solutions in dependence of pH and temperature. Cloud point measurements indicated the formation of larger aggregates at pH 4.5 and temperatures above the lower critical solution temperature (LCST) of PNIPAAm. The solution behavior is strongly influenced by hydrogen bonding interactions between the NIPAAm and acrylic acid blocks.

Introduction

Block copolymers consisting of poly(acrylic acid), PAA, and poly(*N*-isopropylacrylamide), PNIPAAm, are of interest for a variety of reasons. First of all, poly(acrylic acid) is a polymer that responds to changes in pH and ionic strength with changes in its properties; e.g., at pH < 4 precipitation occurs in aqueous solutions due to protonation of the carboxylate groups, which renders the polymer sparsely soluble in water. Poly(*N*-isopropylacrylamide), PNIPAAm, shows lower critical solution temperature (LCST) behavior in aqueous solutions, and a sharp phase transition is observed at 32 °C in water.¹

The combination of pH-responsive PAA and temperature-responsive PNIPAAm creates systems that respond to combined external stimuli. Conjugation of drugs or proteins to PNIPAAm-*b*-PAA generates thermo- and pH-responsive entities that can be addressed through external stimuli.

Furthermore, PNIPAAm-*b*-PAA may form micelles or other aggregates depending on solvent, temperature, pH, and block lengths (cf. Figure 1). Temperature- or pH-sensitive micelles could eventually be used to confer bioadhesive properties; pH-sensitive micelles might be applied in the drug delivery to tumors, inflamed tissues, or endosomal compartments, where a pH lower than that in normal tissue is found.²

For that reason, we synthesized the corresponding block copolymers by reversible addition–fragmentation

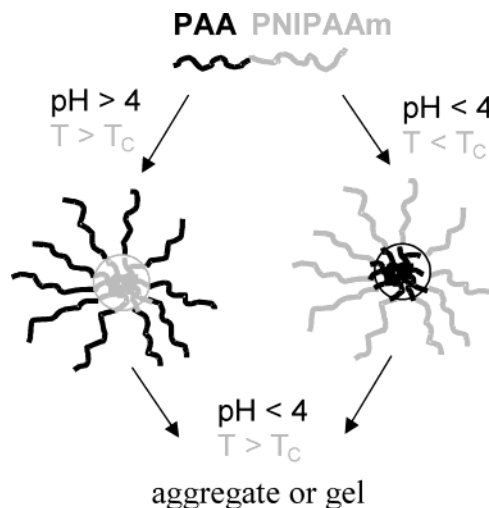


Figure 1. Possible modes of aggregate formation for PNIPAAm-*b*-PAA in aqueous solution in dependence of pH and temperature.

chain transfer (RAFT) polymerization of NIPAAm in the presence of a PAA RAFT agent synthesized earlier.³ We investigated the behavior of these block copolymers in DMF and aqueous solution using turbidimetry, dynamic light scattering, cryogenic transmission electron microscopy, Raman and IR spectroscopy.

Experimental Section

Materials. *N*-Isopropylacrylamide (Aldrich, 97%) was recrystallized twice from benzene/hexane 3:2 (v:v) and dried under vacuum prior to use. Azobis(isobutyronitrile) (AIBN, Fluka, purum) was recrystallized twice from methanol. Poly(acrylic acid) (polymeric RAFT agent) was obtained from RAFT

* Corresponding author. Fax: +49-921-553393. E-mail: axel.mueller@uni-bayreuth.de.

[†] Universität Bayreuth.

[‡] CSIRO Molecular Science.

[§] Uppsala University.

Table 1. Experimental Conditions and Results of the Block Copolymerization of PAA with PNIPAAm (1.5 M) Using PAA (DP_n = 110, M_n = 7900 g/mol, M_w/M_n = 1.19) as Macromolecular Chain Transfer Agent in Methanol at 60 °C

entry	PAA (mM)	AIBN (mM)	time (h)	convn (%)	10 ⁻⁴ M _{n,theor} (g/mol)	10 ⁻⁴ M _{n,MALDI} (g/mol)	n ^c	10 ⁻⁴ M _{n,GPC} ^a (g/mol)	M _w /M _n
1	14.8	7.0	10	64	1.51	1.36	50	22.8 (237) ^b	1.11
2	14.8	7.0	16	82	1.72	1.40	54	26.6 (275) ^b	1.09
3	9.4	7.0	16	48	1.65	1.63	74	22.2	1.06
4	13.0	4.6	10	75	1.77	1.43	57	8.57	1.15
5	6.5	4.6	10	65	2.49	2.34	137	29.2	1.03

^a In DMF/LiBr with PMMA calibration. ^b Absolute molecular weights using a light scattering detector. ^c DP_n of PNIPAAm block, $n = (M_{n,MALDI} - M_{n,PAA})/M_{NIPAAm}$.

polymerization of acrylic acid in methanol with 1-cyanoethyl 2-pyrrolidone-1-carbodithioate as chain transfer agent.³ It was purified by precipitating its methanol solution into ethyl acetate in order to remove residual monomer and to avoid formation of gradient copolymers in the subsequent block copolymerization with NIPAAm. The precursor had M_n = 7900 g/mol (DP_n = 110) and M_w/M_n = 1.19.

Polymerizations. RAFT polymerizations were carried out in methanol as solvent using AIBN as initiator at 60 °C. NIPAAm (1.5 mol/L) and the other reagents (for concentrations see Table 1) were mixed in a vial and aliquots were transferred to ampules, which were degassed by three freeze–thaw–evacuate cycles and then flame-sealed under vacuum. The ampules were immersed completely in an oil bath at the specified temperature.

Analyses. Gel permeation chromatography (GPC) of the DMF-soluble PNIPAAm-*b*-PAA was performed using a series of four Styragel columns HT2, HT3, HT4, and HT5 and an oven temperature of 80 °C. The solvent was DMF + 0.05 M LiBr at a flow rate of 1.0 mL/min. A Dawn EOS light scattering detector with Optilab DSP interferometer (both set at 690 nm) was used.

GPC using water + 0.05 M sodium azide was conducted on PSS Suprema columns (300 × 8 mm, 10 μm particle size) with 10², 10³, and 10⁴ Å pore sizes. Poly(methacrylic acid) standards were used for calibration. The measurements were carried out at a flow rate of 1 mL/min at 25 °C or 60 °C, respectively, using RI and UV detection (λ = 254 nm).

MALDI–TOF mass spectrometry was performed on a Bruker Reflex III spectrometer equipped with a 337 nm N₂ laser in the reflector mode and 20 kV acceleration voltage. Sinapinic acid (Aldrich, 97%) was used as the matrix material. No salt addition was necessary. Samples were prepared from ethanol solution by mixing matrix (20 mg/mL) and sample (10 mg/mL) in a ratio of 10:1. The number-average molecular weights, M_n, of the polymer samples were determined in the linear mode.

Dynamic light scattering (DLS) was performed on an ALV DLS/SLS-SP 5022F compact goniometer system with an ALV 5000/E correlator and a He–Ne laser (λ = 632.8 nm). The polymer solutions were prepared from 0.1 M citrate buffered aqueous solutions with polymer concentration c ≈ 1.1 mg/mL. The solutions were filtered twice through Millipore nylon filters (pore size 0.45 μm). The normalized intensity autocorrelation function g₂(t) was measured experimentally. The CONTIN method was used for data analysis of g₂(t). The following nonlinear fit model was used:

$$g_2(t) - 1 = \left(\int_{t_{\min}}^{t_{\max}} e^{-t} G(t) dt \right)^2$$

G(t) denotes the decay rate distribution function. This analysis results in a discrete, intensity-weighted distribution function of logarithmically equidistant-spaced decay time. The hydrodynamic radii were calculated from the corresponding decay time applying the Stokes–Einstein equation, based on the assumption that the scattering particles behave as hard spheres in dilute solution and within the Rayleigh–Debye theory.

IR spectra were recorded on a Bruker Equinox 55/S FT-IR spectrometer. The measurements were performed on films on CaF₂ plates cast from aqueous solutions.

Raman spectra were recorded using a confocal optical setup consisting of a He–Ne laser (λ = 632.8 nm), objectives of numerical aperture 0.45 and 0.20, and a 50 μm pinhole replacing the entrance slit of the monochromator. A CCD line detector in the exit focal plane of the monochromator was used for recording the spectra.

Cloud point measurements were performed in 0.2 wt % (buffered) aqueous polymer solutions. For details, see ref 3.

Cryogenic transmission electron microscopy (cryo-TEM) measurements were performed on a Zeiss EM 902A instrument with operation in the zero-loss bright-field mode and an acceleration voltage of 80 kV. Digital images were recorded with a BioVision Pro-SM Slow Scan CCD camera system. A climate chamber was used for sample preparation in order to control temperature and relative humidity. The temperature was set to 25 or 45 °C, respectively, and the relative humidity was set to 99%. Samples were prepared by placing a drop of the aqueous solution on a copper grid, which was covered with a perforated polymer film and coated with carbon on both sides. The sample film was thinned by blotting and was vitrified in liquid ethane.

Results and Discussion

PNIPAAm-*b*-PAA was synthesized by the RAFT process for the first time. The block copolymerization was performed using poly(acrylic acid) as a macromolecular chain transfer agent. The obtained polydispersities are very low. Table 1 summarizes the results obtained for block copolymers with a PAA block length equal to 110 monomer units.

MALDI–TOF mass spectrometry, used for determination of number-average molecular weights, led not only to singly charged but also to multiply charged molecules due to the ease of ionization of the acrylic acid blocks. In general, two major peaks were found in the MALDI–TOF spectra, which were attributed to single- and double-charged polymers.

Both DMF and water were used as solvents for GPC to determine molecular weight averages and polydispersities of the block copolymers from entries 1 and 2 in Table 1. In all cases, the molecular weights determined by GPC are about one order of magnitude higher than the theoretical and MALDI values. Light scattering detection yields even higher values (entries 1 and 2 in Table 1). This was attributed to the formation of aggregates in solution and will be discussed along with further details on aqueous GPC. It was also confirmed by ¹H NMR in DMF-*d*₇.³

In the following, the characteristics of block copolymers with a fixed AA block length of 110 units and a varying NIPAAm block length of *n* units is discussed, and polymers will be abbreviated as (NIPAAm)_{*n*}-*b*-(AA)₁₁₀.

Gel permeation chromatography with DMF as eluent, using a light scattering detector, was used to evaluate the molecular weights of the block copolymers. The obtained M_n values were about two orders of magnitude

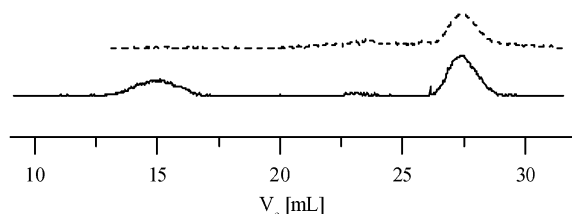


Figure 2. GPC traces (RI detector) of (NIPAAm)₅₀-*b*-(AA)₁₁₀ at 25 (top) and 60 °C (bottom) in water + 0.05 M NaN₃.³

higher than the calculated ones. Therefore, it was assumed that aggregation takes place. This is not quite expected as DMF should be a good solvent for both the PNIPAAm and the PAA block. To prove this assumption, aqueous GPC of the polymer samples was performed at 25 and 60 °C. At 25 °C, only one peak is observed, whereas two peaks were found at 60 °C, namely one in the high-molecular weight region and one at the same elution volume as the peak observed at 25 °C (Figure 2). The absence of a peak at higher elution volume at 25 °C indicates the absence of homo-PAA or homo-PNIPAAm.

This observation strongly indicates the formation of micelles at 60 °C, which is above the cloud point of PNIPAAm. At this temperature, PNIPAAm is insoluble in aqueous solution, and it is assumed that it forms the core of a micelle with PAA forming the corona (Figure 1). Micelle formation at elevated temperature was also confirmed by dynamic light scattering (see below). Thus, the peak at lower elution volume in Figure 2 corresponds to micelles.

The combination of pH-responsive poly(acrylic acid), PAA, and thermoresponsive poly(*N*-isopropylacrylamide), PNIPAAm, in a block copolymer leads to a system that responds to both pH and temperature. The solubility of the PAA block in aqueous solutions depends on the pH of the medium. The lower the pH, the more carboxylate groups of the PAA blocks are protonated and the less soluble this block becomes in aqueous media. At pH > 8, virtually all carboxylate groups are deprotonated, and the PAA segment is readily soluble in water. From the PNIPAAm point of view, its LCST is altered through the attachment of acrylic acid chains and it is expected to be raised if the acrylic acid block is hydrophilic and lowered if the acrylic acid block is hydrophobic. In some cases, LCST behavior can even be lost if the length of the acrylic acid block is too large.⁴

The influence of different pH values on the cloud point, T_c , was investigated on 0.2 wt % buffered aqueous solutions with pH values ranging from 7 to 4.5. For pH = 5.0–7.0, 0.1 M phosphate buffer and for pH = 4.5–5.0, 0.1 M citrate buffer were used. No influence of the type of buffer (phosphate or citrate buffer) on the appearance of the turbidimetric curves was found so that small differences in ionic strength owing to the different buffer systems can be neglected.

Figure 3 shows the turbidimetric curves of PNIPAAm-*b*-PAA at different pH values. The transmission decreases only slightly at pH values 5.0–7.0 when the temperature is raised above the LCST of PNIPAAm. This suggests the presence of micelles with PNIPAAm forming the micellar core at $T > T_c$ and PAA forming the corona. Dynamic light scattering confirms these findings (see following section). At pH 4.5, transmission decreases to 0% when the temperature is raised above T_c , indicating the formation of larger aggregates due to increasing insolubility of the protonated PAA corona.

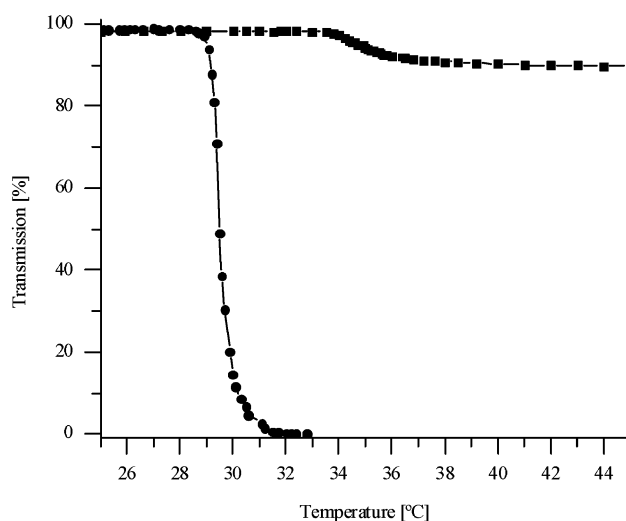


Figure 3. Turbidimetry of buffered aqueous solutions of (NIPAAm)₅₀-*b*-(AA)₁₁₀: (●) pH 4.5; (■) pH 5–7.³

Consequently, the formation of this type of micelles is dependent on both pH and temperature. Such a doubly responsive behavior in aqueous media has also been described by Armes et al. for the system poly(2-diethyl-aminoethyl methacrylate)-*block*-poly(propylene oxide)⁵ and by Laschewsky et al. for poly(2-[*N*-(3-methacrylamidopropyl)-*N,N*-dimethyl]ammoniopropanesulfonate)-*block*-poly(*N*-isopropylacrylamide).⁶

Figure 3 also shows that the cloud point of PNIPAAm is raised from $T_c = 32$ °C for the pure polymer to ca. 35 °C at pH 5–7, whereas it is slightly lowered to ca. 29 °C at pH 4.5. This is due to acrylic acid segments that are hydrophilic at pH 5–7 and thereby increase the cloud point, but the acrylic acid segments are relatively hydrophobic at pH 4.5 due to protonation of the carboxylate groups, which decreases T_c .

Dynamic light scattering (DLS) measurements were performed on buffered aqueous solutions of PNIPAAm-*b*-PAA of pH 5.6 at different temperatures. The typical field correlation functions are shown in Figure 4. At 20 °C $\leq T \leq 35$ °C, three peaks are found in the intensity-weighted (z) hydrodynamic radius distribution function (Figure 5, top), which are believed to correspond to unimers, aggregates, and larger aggregates. Since the CONTIN analysis renders intensity-weighted distributions, the proportion of the large particles is strongly exaggerated, as the scattering intensity is strongly dependent on the radius of the particle ($\sim R^6$ for spherical particles). Thus, the weight fraction of the aggregates is actually rather small. In a corresponding mass distribution plot, $w(\log R_h) \sim z(\log R_h)/R_h^3$, the peak for the unimer is dominant along with a small peak for aggregates located at $R_h \sim 20$ nm, and the peak for large aggregates ($R_h > 100$ nm) almost disappears. The nature of the aggregates will be discussed below.

With increasing temperature, the scattering intensity was observed to be nearly constant within the temperature range of 20 °C $\leq T \leq 35$ °C. When the temperature was increased to 42 °C, which is above T_c of PNIPAAm in the block copolymer, there was a dramatic increase in the scattering intensity (more than two times). At this temperature a bimodal distribution is found in the intensity-weighted hydrodynamic radius distribution function and the unimer peak disappears. Additionally, the peak at $R_h \sim 20$ nm is dominant in this case. When the temperature increased to 50 °C, the

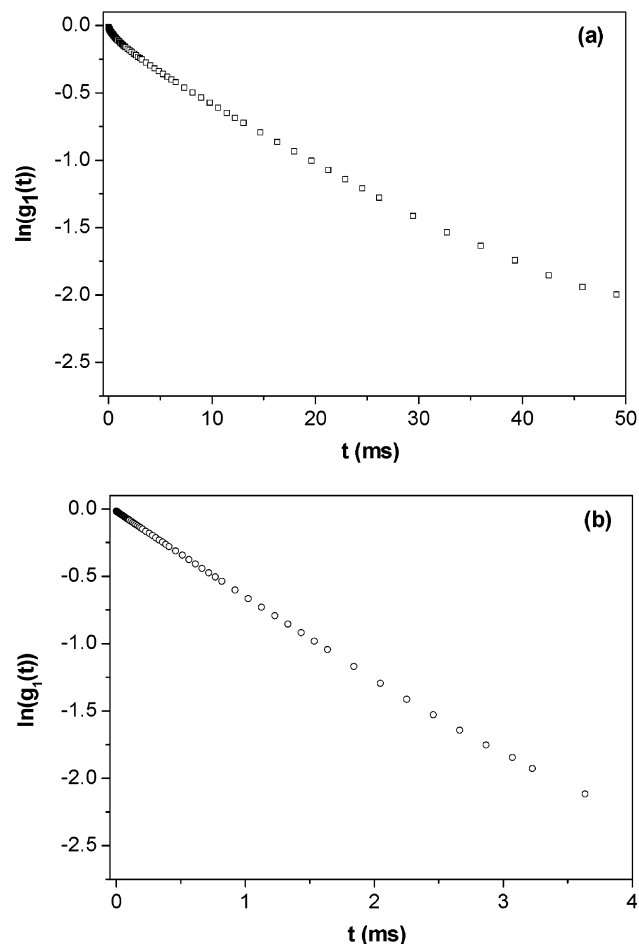


Figure 4. Field correlation functions of (NIPAAm)₇₄-*b*-(AA)₁₁₀ in 0.1 M citrate buffer pH 5.6 at a scattering angle of 30°: (a) $T = 35\text{ }^{\circ}\text{C}$; (b) $T = 50\text{ }^{\circ}\text{C}$.

scattering intensity increased further (about 1.5 times of that at 42 °C), and only one very narrow peak is observed in the hydrodynamic radius distribution curve (Figure 5, bottom). In this case, micelles with hydrophobic PNIPAAm constituting the micellar core and hydrophilic PAA forming the corona are most likely formed.

DLS suggests the formation of aggregates at room temperature as the hydrodynamic radii of the particles are smaller than those of the micelles observed at higher temperature but too large for unimers. In the literature, hydrogen-bonded interpolymer complexes between poly(acrylic acid) and poly(acrylamide) derivatives have been reported, where acrylamide acts as a strong hydrogen acceptor and acrylic acid provides hydrogen for binding.^{7,8} Taking these findings into consideration, it can be assumed that intermolecular hydrogen bonding takes place between PAA and PNIPAAm. To prove hydrogen bonding between amide and carboxylic acid, Shibamura et al. applied FT-IR spectroscopy using the ATR (attenuated total reflectance) technique that allows for measurement in aqueous solutions.^{8,9} In this work, Raman spectroscopy was considered as a substitute for the ATR technique. One of the advantages of Raman spectroscopy is that water can be used as a solvent, which is almost impossible in IR transmission spectroscopy due to the strong absorption of water. Raman spectroscopy is usually best suited for the characterization of nonpolar or only slightly polar bonds. The strong and characteristic IR bands of polar groups, such as C=O or O-H,

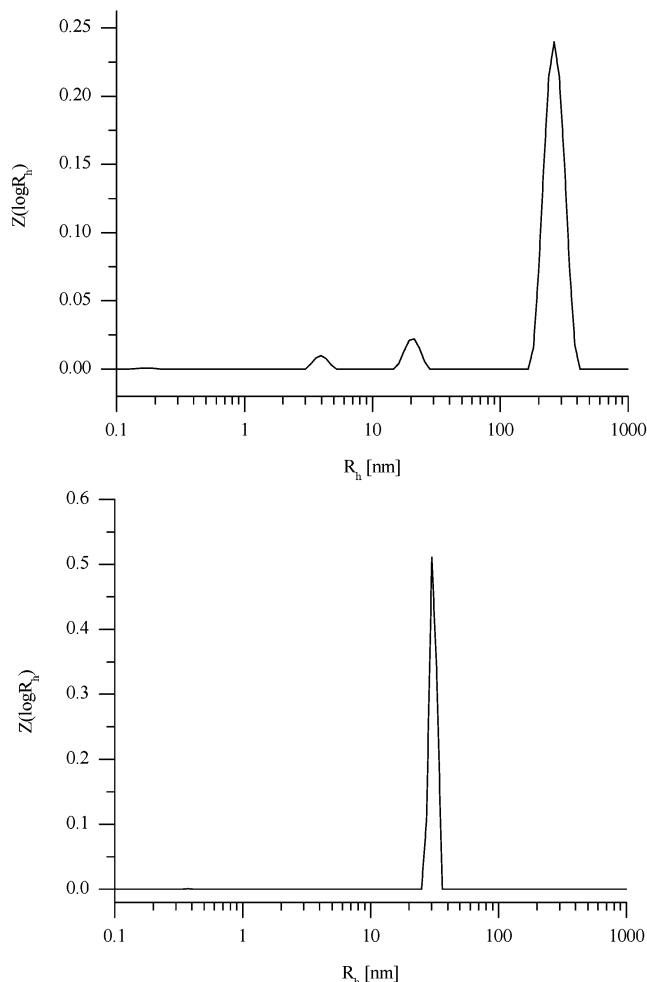


Figure 5. Hydrodynamic radii distribution of (NIPAAm)₇₄-*b*-(AA)₁₁₀ in 0.1 M citrate buffer pH 5.6 (CONTIN analysis; $\theta = 30^{\circ}$). Top: $T = 35\text{ }^{\circ}\text{C}$. Bottom: $T = 50\text{ }^{\circ}\text{C}$.

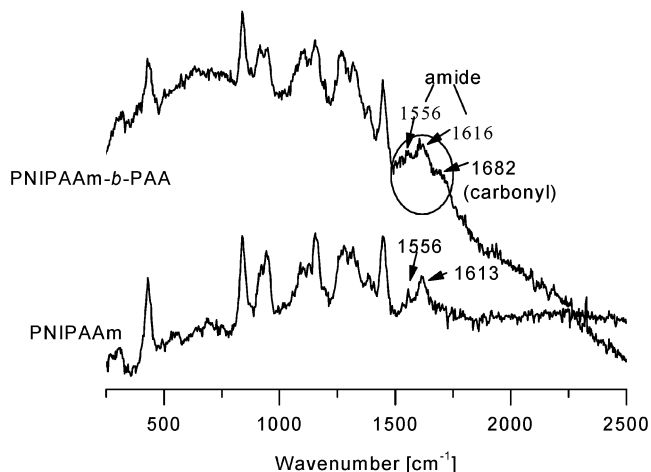


Figure 6. Raman spectra of aqueous solutions of (NIPAAm)₁₃₇-*b*-(AA)₁₁₀ at pH 6 and of PNIPAAm.

are usually reduced in the Raman spectra so that relatively weak carbonyl stretching bands are expected.¹⁰

Figure 6 shows the Raman spectrum obtained for a 2 wt % solution of PNIPAAm-*b*-PAA in citrate buffer pH 5.6 along with that of a 2 wt % aqueous PNIPAAm solution for comparison. To eliminate buffer signals, pure 0.1 M citrate buffer was recorded and the spectrum was subtracted from the Raman spectrum of the block copolymer.

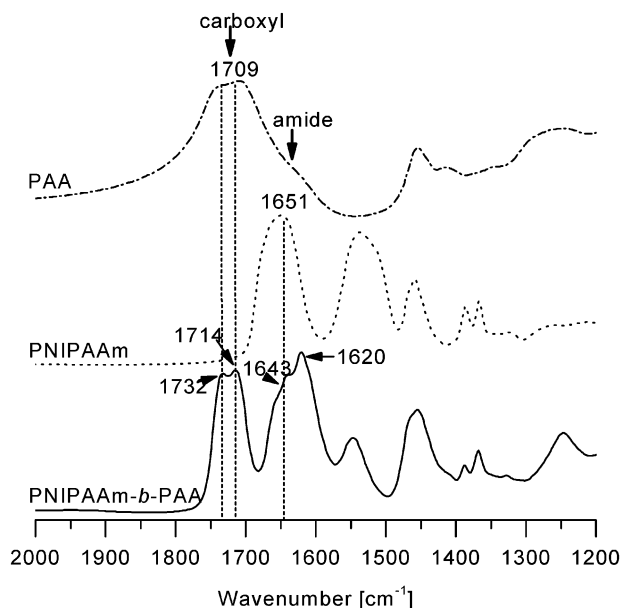


Figure 7. IR spectrum of solid $(\text{NIPAAm})_{137}\text{-}b\text{-(AA)}_{110}$ with spectra of the homopolymers PNIPAAm and PAA for comparison.

The carbonyl and amide stretching bands in the Raman spectrum appear at a somewhat lower wavenumber as compared to IR spectroscopy. The respective stretching bands are relatively weak, as was expected for a polar group in Raman spectroscopy. Comparing the spectrum of the homopolymer PNIPAAm with that

of the block copolymer PNIPAAm-*b*-PAA, the bands at 1556 and 1613 cm^{-1} in the PNIPAAm spectrum were attributed to amide stretching, which is found at 1556 and 1616 cm^{-1} in the block copolymer spectrum. The band at 1682 cm^{-1} arises from carbonyl stretching of the acrylic acid carboxyl groups in PNIPAAm-*b*-PAA. On comparison of the stretching bands in the PNIPAAm and PNIPAAm-*b*-PAA spectra, it is evident that the stretching bands in the block copolymer spectrum are broadened with respect to the PNIPAAm spectrum. This is an indication for some complexation or hydrogen bonding taking place between the two blocks. Such a broadening of stretching bands due to cooperative $\text{H}\cdots\text{O}$ interactions has also been observed by other authors.¹¹

To confirm the conclusion drawn from the Raman spectra, IR spectroscopy was used on block copolymer samples that were cast on calcium fluoride plates from 2 wt % aqueous phosphate-buffered solutions. Figure 7 shows an exemplary IR spectrum as compared with those of the homopolymers.

On comparison of the different spectra, a splitting of the amide stretching band in PNIPAAm-*b*-PAA is evident and the band is shifted to lower wavenumbers, whereas the split carbonyl stretching band of the block copolymer is shifted to higher wavenumbers with respect to the homopolymer spectra. These observations agree with those reported in the literature for hydrogen bonding between acrylic acid and acrylamides.⁸ The carbonyl stretching band in the PAA homopolymer spectrum is already somewhat split due to partial

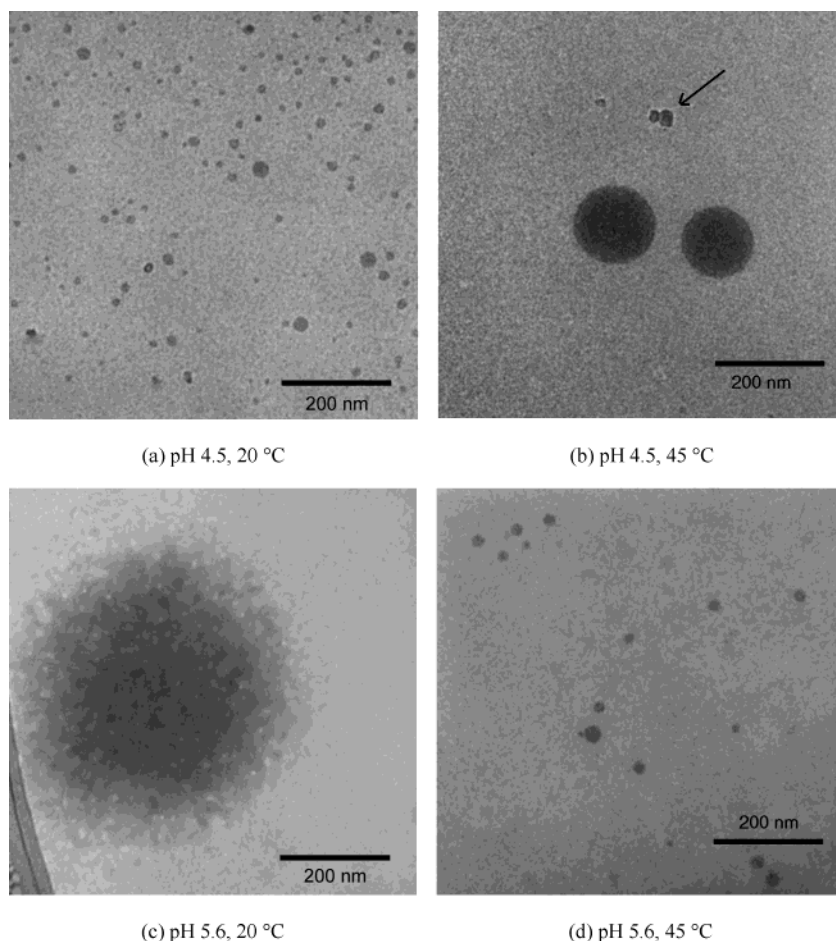


Figure 8. Cryo-TEM images for $(\text{NIPAAm})_{74}\text{-}b\text{-(AA)}_{110}$ cast from buffered aqueous solutions of pH 4.5 or pH 5.6, respectively, at temperatures below and above LCST of PNIPAAm. The arrow denotes an ice crystal attached to the surface after vitrification.

hydrogen bonds between the carboxylic acid groups. This also agrees with results reported in the literature.⁸

In conclusion, interpolymer hydrogen bonding in PNIPAAm-*b*-PAA leads to the formation of aggregates at room temperature. Micelles are formed at temperatures above ca. 40 °C with PNIPAAm forming the micellar core and PAA constituting the corona.

To further investigate the structures of micelles and aggregates in solution, cryogenic transmission electron microscopy (cryo-TEM) measurements were performed on buffered PNIPAAm-*b*-PAA solutions of pH 4.5 and pH 5.6 at 20 °C and 45 °C. These temperatures were chosen to study the solutions below and above the LCST of PNIPAAm. Figure 8 shows the corresponding cryo-TEM images.

The transmission electron micrograph at pH 4.5 and 20 °C (Figure 8a) shows particles of diameters in the range of 10–30 nm, which might correspond to micelles with PAA core. From the size and fact that these particles sometimes touch each other (e.g., in the upper right part of the image) one may conclude that not only the core but also the shell is seen. Some smaller structures can be observed but their size cannot be quantified due to lack of sufficient contrast. At pH 4.5 and 45 °C (b), large particles with diameters of about 130 nm are seen in the micrographs. These are assigned to larger aggregates. No hydrogel formation seems to take place (also confirmed by the low viscosity) as one might have expected due to the insolubility of both PNIPAAm and PAA at high temperature and low pH values. Hydrogel formation may require a higher concentration than that of 2 wt %, which was used for the block copolymer solutions and will occur more easily with ABA triblock copolymers.

The transmission electron micrograph at pH 5.6 and 20 °C shows large aggregates ($d > 300$ nm) and barely visible, smaller particles, confirming the DLS results that indicated aggregates of different sizes. The smallest particles observed in the DLS studies are invisible due to lack of sufficient contrast in the images. At pH 5.6 and 45 °C, aggregates of diameters in the range of 10–30 nm are observed. This is in good agreement with DLS measurements, where a coexistence of micelles and unimers was found. Again, small particles, i.e., unimers, are not detected due to the low contrast.

Conclusions

Hydrogen bonding between *N*-isopropylacrylamide and acrylic acid units in PNIPAAm-*b*-PAA block copoly-

mers influences strongly their behavior in solution. The block copolymers form starlike micelles in aqueous solutions in dependence on pH and temperature. Cloud point measurements indicated the formation of larger aggregates at pH 4.5 and temperatures above LCST, whereas micelles formed at pH 5–7 and temperatures above LCST. At pH 5.6 and 50 °C, only micelles were found, whereas at lower temperatures, larger aggregates and micelles coexist. Formation of larger aggregates by hydrogen bonding interactions was revealed by IR and Raman spectroscopy as well as by cryogenic transmission electron microscopy and dynamic light scattering.

Acknowledgment. The authors thank Prof. Lothar Kador and Carmen Perez-Leon, Experimental Physics IV, Universität Bayreuth, for their efforts with Raman spectroscopy and Cornelia Lauble for the MALDI-TOF measurements. This work was supported by the Deutsche Forschungsgemeinschaft (DFG).

References and Notes

- (1) Hsu, S.-H.; Yu, T.-L. *Macromol. Rapid Commun.* **2000**, *21*, 476–480.
- (2) Jones, M.-C.; Leroux, J.-C. *Eur. J. Pharmacol. Biopharm.* **1999**.
- (3) Schilli, C.; Müller, A. H. E.; Rizzardo, E.; Thang, S. H.; Chong, B. Y. K. In *Advances in controlled/living radical polymerization*; Matyjaszewski, K., Ed.; ACS Symposium Series 854; American Chemical Society: Washington, DC, 2003; pp 603–618.
- (4) Bulmus, V.; Ding, Z.; Long, C. J.; Stayton, P. S.; Hoffman, A. S. *Bioconjugate Chem.* **2000**, *11*, 78–83.
- (5) Liu, S.; Billingham, N. C.; Armes, S. P. *Angew. Chem., Int. Ed.* **2001**, *40*, 2328–2331.
- (6) Arotcarena, M.; Heise, B.; Ishaya, S.; Laschewsky, A. *J. Am. Chem. Soc.* **2002**, *124*, 3787–3793.
- (7) Wang, Y.; Morawetz, H. *Macromolecules* **1989**, *22*, 164–167.
- (8) Shibamura, T.; Aoki, T.; Sanui, K.; Ogata, N.; Kikuchi, A.; Sakurai, Y.; Okano, T. *Macromolecules* **2000**, *33*, 444–450.
- (9) Ramon, O.; Kesselman, E.; Berkovici, R.; Cohen, Y.; Paz, Y. *J. Polym. Sci., Part B: Polym. Phys.* **2001**, *39*, 1665–1677.
- (10) Hesse, M.; Meier, H.; Zeeh, B. *Spektroskopische Methoden in der organischen Chemie*, 5th ed.; Georg Thieme Verlag: Stuttgart, Germany, 1995.
- (11) Blatchford, M. A.; Raveendran, P.; Wallen, S. L. *J. Am. Chem. Soc.* **2002**, *124*, 14818–14819.

MA035838W